ACS APPLIED MATERIALS & INTERFACES

Research Article

www.acsami.org

# Reversible Superhydrophobic–Superhydrophilic Transition of ZnO Nanorod/Epoxy Composite Films

Yan Liu,[†] Ziyin Lin,[†] Wei Lin,[†] Kyoung Sik Moon,[†] and C. P. Wong*[,†,‡]

[†]School of Materials Science and Engineering, Georgia Institute of Technology, 771 Ferst Drive, Atlanta, Georgia 30332-0245, United States

[‡]Faculty of Engineering, The Chinese University of Hong Kong, Shatin, NT, Hong Kong

**ABSTRACT:** Tuning the surface wettability is of great interest for both scientific research and practical applications. We demonstrated reversible transition between superhydrophobicity and superhydrophilicity on a ZnO nanorod/epoxy composite film. The epoxy resin serves as an adhesion and stress relief layer. The ZnO nanorods were exposed after oxygen reactive ion etching of the epoxy matrix. A subsequent chemcial treatment with fluoroalkyl and alkyl silanes resulted in a superhydrophobic surface with a water contact angle up to 158.4° and a hysteresis as low as 1.3°. Under UV irradiation, the water contact angle decreased gradually, and the surface eventually became superhydrophilic because of UV induced decomposition of alkyl silanes and hydroxyl absorption on ZnO surfaces. A reversible transition of surface wettability was realized by alternation of UV illumination and surface treatment. Such ZnO nanocomposite surface also showed improved mechanical robustness.

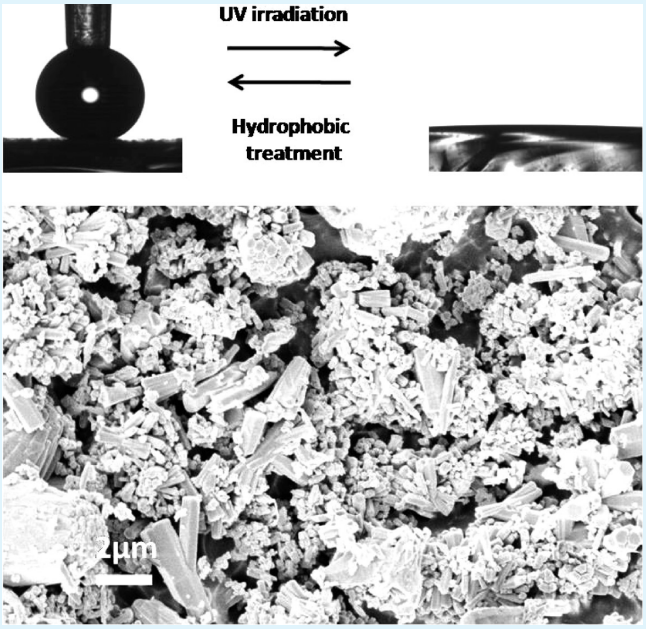


**KEYWORDS:** *reversible wettability, ZnO nanocomposite films, UV irradiation*

## INTRODUCTION

Suface wettability, an important property for solid materials, has been known to be controlled by surface energy and morphology.[1−4] Modifying the surface wettability is very important for chemical and electronic applications, such as inkjet printing,[5] microfluid channels,[6] etc. For those practical applications, both superhydrophobic (water contact angle (CA) larger than 150°) and superhydrophilic surfaces (water CA is almost 0°) are very useful.[7−9] Recently, materials with tunable wettability have been developed and realized on many inorganic oxide surfaces, such as $TiO_2$, ZnO, $WO_3$, $V_2O_5$, and $SnO_2$.[10−13] Under UV irradiation, the hydrophobic/superhydrophobic oxide surfaces turns hydrophilic/superhydrophilic. In the dark, the surface turns back to hydrophobic/superhydrophobic.[10] Tunable wettability was also reported on polymers, metal oxides, and semiconductors under UV or visible light illumination.[14−17]

With a direct wide band gap of 3.37 eV and a large exciton binding energy of 60 meV at room temperature, ZnO has been demonstrated to have enormous applications in electronic and optoelectronic devices, such as ultraviolet (UV) lasers,[18,19] light-emitting diodes,[20] field-emission devices,[21,22] nano generators,[23,24] and solar cells.[25,26] One-dimensional (1D) ZnO nanostructures can be synthesized by a wide range of techniques including vapor deposition, electrodeposition, hydrothermal method, molecular beam epitaxy, and so on.[27] Among these methods, hydrothermal method has been widely used due to its low cost and scalability .[28] Many papers have been reported about creating superhydrophobic surfaces with 1D ZnO nanostructures (nanowires, nanorods, nanofibers).[28,29] Reversed wettability has been reported on those ZnO nanostructure films.[30−34] For example, Feng et al. reported superhydrophobic to superhydrophilic of aligned ZnO nanorod films switched by alternation of UV irradiation and dark storage.[35] Kwak et al. grew superhydrophobic ZnO nanowire surface modified by fatty acids, and switched to hydrophilic under UV irradiation.[36] A selective UV photopatterning of ZnO nanowire film with different wettability was realized.

However, most previous research has been focused on wettability investigation of ZnO nanostructure itself; until now,

Received: May 3, 2012
Accepted: July 5, 2012
Published: July 5, 2012

  

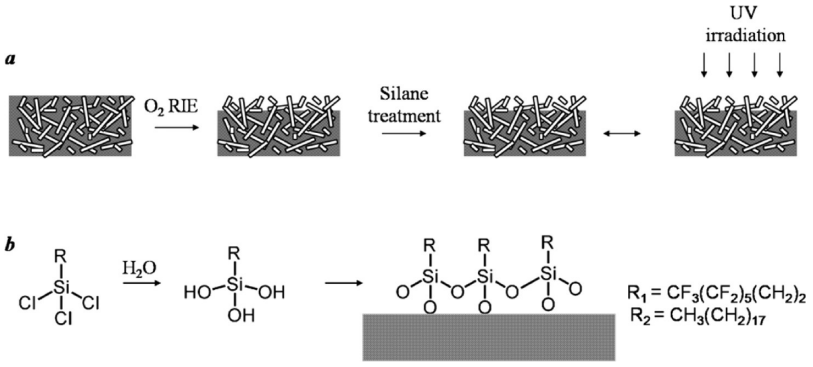


**Figure 1.** (a) Schematic of the fabrication process for superhydrophobic ZnO nanorod composite film and its transition to superhydrophilic film under UV irradiation (b) PFOS and OTS silane treatment on ZnO nanorod composites.

no paper has been reported about preparing ZnO nanocomposites with tunable wettability. For most of superhydrohobic surfaces made of inorganic materials, the surface micro- and nano- structures are prone to mechanical damage under abrasion forces due to their brittle nature. Therefore a protective polymeric material such as epoxy resin, could be introduced as an adhesion and stress relief layer to the substrate. The inorganic nanoparticles at the surface of the polymeric layer generates an abrasion resistant surface layer. The resulting nanocomposite is also easier to be applied by various methods such as spin coating, spraying and printing techniques. In this study, ZnO nanorods were synthesized by hydrothermal method, and mixed with epoxy resins of different filler loadings. After oxygen reactive ion etching (RIE), the top epoxy was etched and ZnO-based hierarchical structure was exposed. Superhydrophobic ZnO film could be produced after surface modification for lowering down the surface energy. The ZnO nanocomopposite surface showed better mechanical robustness than the previously reported superhydrophobic surface with inorganic silica nanoparticles. Tunable wettability of superhydrophobicity and superhydrophilicity was realized through UV irradiation and surface functionalization.

## EXPERIMENTAL SECTION

**ZnO Nanorod Growth and Surfactant Treatment.** The growth solution of ZnO nanorods is composed of 5 mmol/L of zinc nitrate hexahydrate and hexamethylenetetramine (HMTA) at a mole ratio of 1:1. The reaction was carried out at 80 °C for 6 h. After reaction, the nanorods were collected using centrifugation and rinsed repeatedly by ethanol. Then the nanorods were baked in oven at 60 °C overnight.

The solution of ethanol and water (95:5 by weight) is adjusted to pH 4.5−5.5 with acetic acid. Aminoethylaminopropyltrimethoxysilane is added with stirring for 5 min to yield a 2 wt % final concentration. ZnO nanorods were silylated by stirring them in solution for 5 min and then decanting the solution. The ZnO nanorods were rinsed twice with ethanol. The silane layer was cured at 110 °C for 10 min.

**ZnO Nanorods/Epoxy Resin Composites.** The epoxy resin was composed of bisphenol A epoxy resin (EPON 828) and ERL 4221 with weight ratio of 1:2. The curing agent HMPA was added with a weight ratio of 1:0.88 to the epoxy resins. Imidazole serves as a catalyst with 1 wt % to the total weight of epoxy resin and curing agent. Then the ZnO nanorods were added into the epoxy resin and mixed by unltrasonication. ZnO nanorod/epoxy composites were prepared at different filler loadings of 17, 33, and 50 wt %. After that, ZnO nanorod film was coated on a glass slide by doctor blade with a thickness of 70 $\mu$m. The glass slide was pretreated by UV-ozone for 5 min. The film was cured at 150 °C in air for 2 h.

**Plasma etching and hydrophobic treatment.** The oxygen RIE was conducted on ZnO nanorod film for 15 min. The power is 150 W and the pressure is 0.5 Torr. Surface modification was performed by immersing coated glass slides in a hexane solution of 3 mM perfluorooctyl trichlorosilane (PFOS) or octadecyltrichlorosilane (OTS) for 30 min, followed by a heat treatment at 150 °C in air for 1 h.

**Abrasion Resistance Test.** In order to evaluate the abrasion resistance of the surfaces, the methodology was previously reported by Xiu et al.[8] Polyester/cellulose Technicloth II wipes served as abrasion surfaces, with the superhydrophobic surface to be tested facing this abrasion material. While a pressure (~3450 Pa) was applied normal to the superhydrophobic surface, the surface was moved in one direction. The contact angle and hysteresis changes of the superhydrophobic surface were then measured after abrasion (25 cm in abrasion length).

**UV Irradiation and Surface Characterization.** UV irradiation was obtained from a 150W Hg arc-lamp. The arc-lamp emission was supplied at a distance of 10 cm and wavelength between 248 and 365 nm. CA measurements were performed with a Rame-Hart goniometer that had a CCD camera equipped for image capture. The deionized water droplet volume was 4 $\mu$L, and the measurements were taken under ambient atmospheric conditions. X-ray diffraction (XRD) analysis was carried out with a Philips X-pert alpha-1 diffactometer, using Cu K$\alpha$ radiation (45 kV and 40 mA). Leo 1530 scanning electron microscope (SEM) was used to characterize the surface morphology of composite samples. Thermo K-Alpha X-ray photoelectron spectroscopy (XPS) was carried out for element composition and analysis.

## RESULTS AND DISCUSSION

Figure 1(a) shows the schematic of fabricating superhydrophobic ZnO nanocomposites. EPON 828 is widely used in surface coatings, adhesives (microelectronics packaging), and composite materials (such as carbon fiber and fiber glass reinforced epoxy). The mixture of EPON 828 with lower viscosity resin ERL 4221 improves the processabilty of ZnO-epoxy composition, especially at high filler loadings. Aminoethylaminopropyltrimethoxysilane is added as a surfactant to improve the interface between nanorods and epoxy matrix. The as synthesized ZnO nanorods have a wide size distribution, which is beneficially for generating micro/nano scale (hierarchical) roughness. After oxygen RIE, the top epoxy resin was etched and the embedded ZnO nanorods were exposed. In order to further reduce the surface energy, two different silane coatings (PFOS and OTS) were applied on the composite surface, by introducing the long hydrocarbon and fluorocarbon chains as shown in Figure 1b. PFOS and OTS were chose to verify the effect of UV light on hydrocarbon and fluorocarbon chains.

The XRD pattern of ZnO nanorods indicates that the as synthesized nanorods are wurtzite ZnO crystals (Figure 2a).

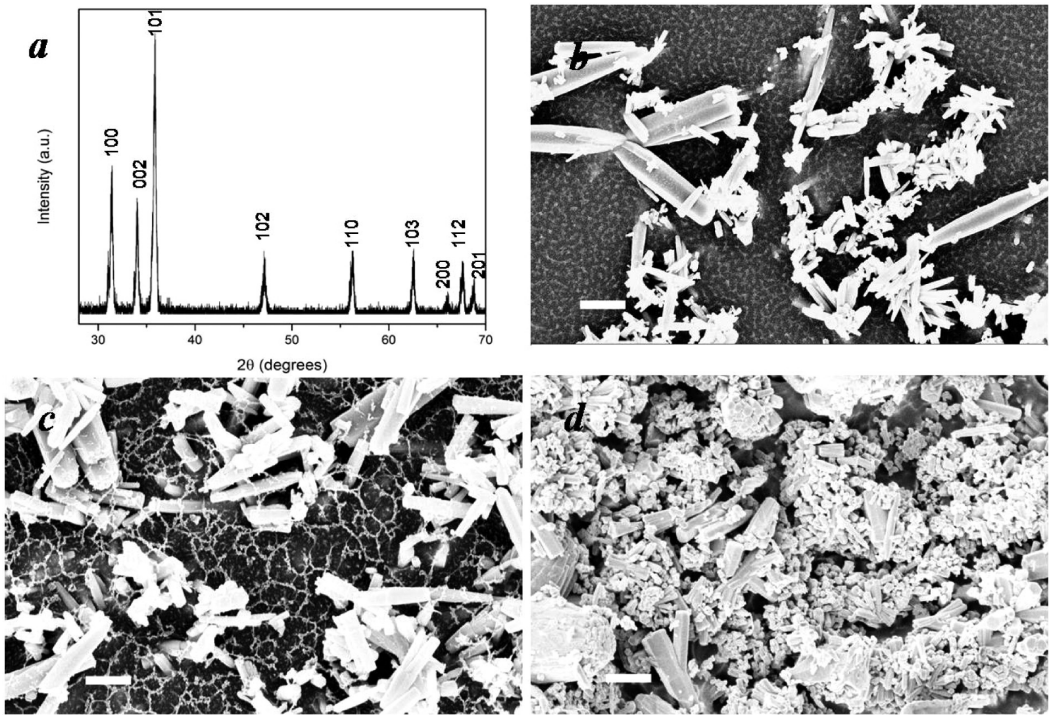


**Figure 2.** (a) X-ray diffraction of ZnO nanorods. (b–d) SEM images of ZnO nanorods composites with different filler loadings after 15 min RIE etching: (b) 17% filler loading, (c) 33% filler loading, (d) 50% filler loading. The scale bar is 2 $\mu$m.

The surface morphologies of composites generated with different filler loadings are shown in Figures 2b–d, where it is evident that the surface roughness increased continuously with the increase of filler loading. Such change yields an increase in water CA and a decrease of CA hysteresis after surface hydrophobic modification by PFOS (Figure 3 and

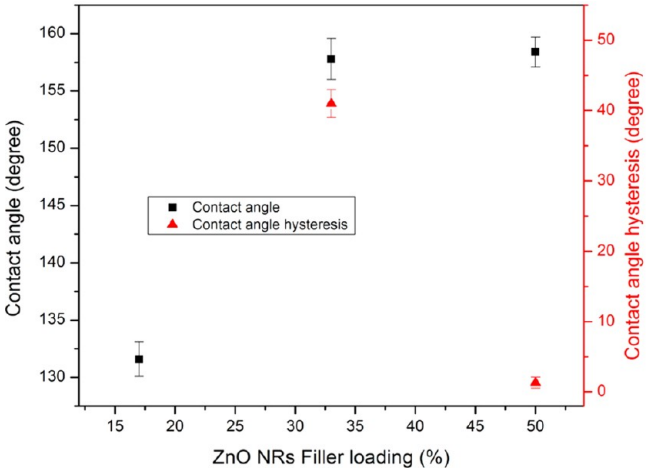


**Figure 3.** Contact angle and contact angle hysteresis of ZnO nanorods composites with different filler loadings (see Table 1).

Table 1). The contact angle of epoxy is 88.4°. After surface treatment of PFOS and OTS respectively, the contact angles became 120.0 and 105.1°. When the filler loading is low (17%), the surface roughness generated is insufficient to construct a superhydrophobic surface. The water CA is only 131.6° ± 1.5°. This low CA could be attributed to the fact that the water droplet makes a wetted contact with the composites, and fills in the grooves on the composite surface. As the filler loading

**Table 1. Contact Angle and Contact Angle Hysteresis of Superhydrophobic Nanocomposites with Different ZnO NR Filler Loadings**

| ZnO NRs filler loading (%) | cntact angles | contact angle hysteresis |
|---|---|---|
| 17 | 131.6 ± 1.5 | |
| 33 | 157.8 ± 1.8 | 41 ± 1.0 |
| 50 | 158.4 ± 1.3 | 1.32 ± 0.2 |

increases to 33%, surface becomes rougher and CA increases to 157.8° ± 1.8°. However CA hysteresis shows a high value of 41° ± 1.0°. When increase the filler loading to 50%, the CA further increase to 158.4° ± 1.3° and CA hysteresis reduced to 1.3° ± 0.2°. The reduced CA hysteresis with increased filler loadings can be explained by the two hydrophobic states on rough solid surfaces, Wenzel and Cassie state. The Wenzel equation,[37] eq 1, describes the effect of surface roughness on the water droplet CA

$$\cos \theta_A = r \cos \theta_Y \quad (1)$$

where $\theta_A$ is the apparent CA on the rough surface, $r$ is the ratio of the actual solid/liquid contact area to its vertical projected area, and $\theta_Y$ is the CA on a flat surface defined by Young's equation. As the roughness ($r$) increases, the CA also increases reflecting an increase in relative hydrophobicity. So when the filler loading changes from 17 to 33%, surface roughness increases, and apparent CA also increases. However, such surface roughness is difficult to trap air between the interface of water droplet and the film surface, and water can easily fill the grooves on the surface, resulting in a large CA hysteresis.

The Cassie equation for a porous or composite surface,[38] eq 2, indicates that the apparent CA increases when the solid surface fraction $f$ decreases. The CA hysteresis in a Cassie state is normally less than 10°

$$\cos\theta_A = -1 + f(\cos\theta_Y + 1) \quad (2)$$

When further increase the filler loading to 50%, ZnO nanorods formed a densely packed layer and enhanced surface roughness significantly. Solid surface fraction decreases, and more air could be trapped at the water and composite interface. The composite surface is composed of both sub micro and nanostructures, such hierarchical structure results in a much reduced CA hysteresis of 1.3°. Air may become trapped between ZnO nanostructures underneath a water droplet, which would further enhance the surface hydrophobicity and reduce the CA hysteresis.

Similarly, we used OTS solution for hydrophobic treatment on 50% loading ZnO nanocomposites. Superhydrophobicity was achieved with a water CA of 152.3° ± 1.2° and CA hysteresis of 2.3° ± 0.6°.

The UV induced wettability change of ZnO nanocomposites is studied by CA measurements and XPS. Under UV irradiation, the water CA of ZnO nanocomposite film by both silane treatments decreased gradually with exposure time, as shown in Figure 4. The CA is reduced abruptly at the

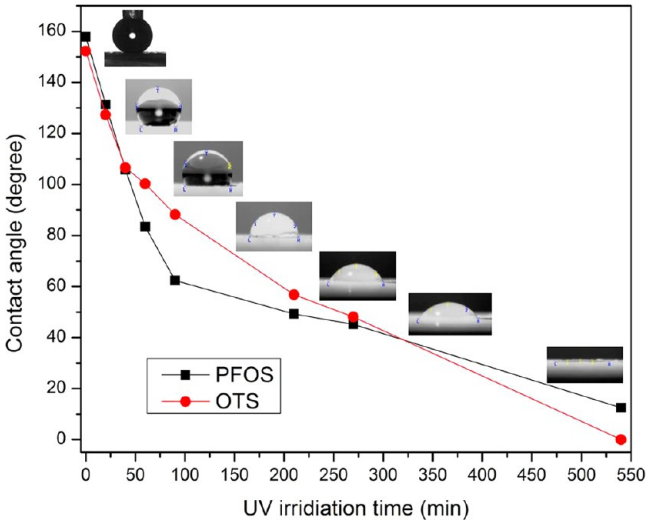


**Figure 4.** Water contact angle of ZnO nanocomposite modified by PFOS and OTS as a function of UV irradiation time.

beginning, because of the high speed yielding of electron−hole pairs at the initial stage under UV irradiation as reported by Liu et al.[30] After 90 min, the change slowed down. After 9 h, the water droplet spread out the film, and CA reaches a low value of ~0° for OTS-treated samples and 12.4° for PFOS-treated samples, indicating the wettability change from superhydrophobicity to superhydrophilicity/highly hydrophilicity. For the PFOS-treated samples, the water CA is higher (12.4°) than the OTS-treated samples after UV irradiation, which may due to the remaining fluorocarbons on the film surface.

The mechanism for superhydrophobicity to superhydrophilicity transition involves the UV effect on both ZnO and silane hydrophobic coatings. Under UV irradiation, the electrons and holes are generated on the ZnO surface. Some of the holes can react with lattice oxygen and form oxygen vacancies. When a surface defective site is generated, water and oxygen may compete to dissociatively adsorb on it. The defective site tends to be kinetically more favorable for hydroxyl absorption than oxygen absorption. This mechansim is supported by XPS results. The Zn $2p_{3/2}$ spectra of ZnO nanocomposites before and after UV irradiation are shown in Figure 5. The Zn $2p_{3/2}$ peaks for ZnO nanocomposites can be deconvoluted into two

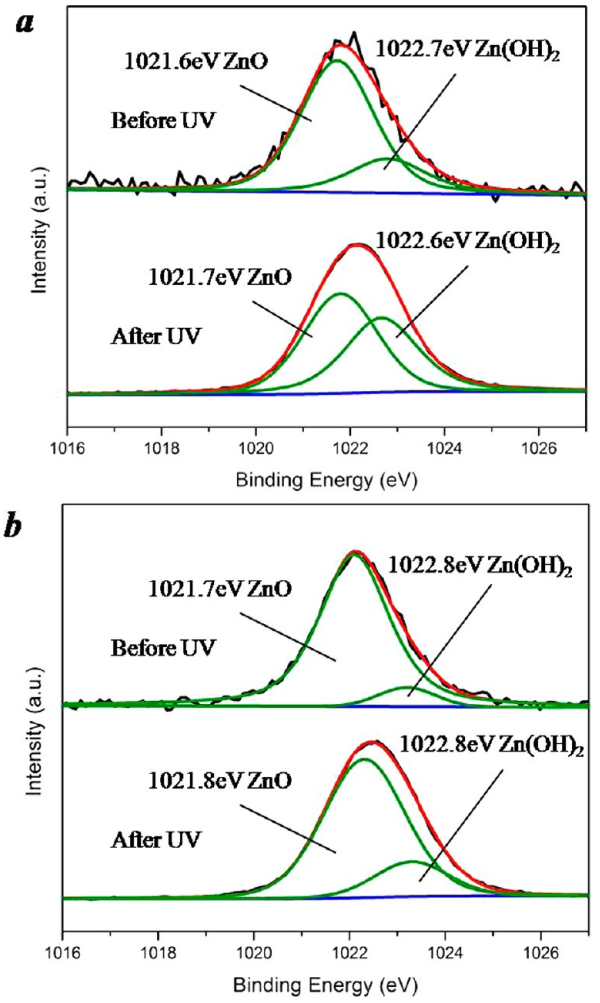


**Figure 5.** XPS spectra of Zn $2p_{3/2}$ of ZnO nanocomposites modified by (a) PFOS, (b) OTS before and after UV irradiation.

compoents at 1021.7 (±0.1) eV and 1022.7 (±0.1) eV, corresponding to to ZnO and $Zn(OH)_2$ respectively. After the UV irradiation for Zn $2p_{3/2}$ spectra, the $Zn(OH)_2$ ratio of PFOS treated composites increases from 22.98% to 45.03%, and $Zn(OH)_2$ ratio of OTS treated samples increases from 7.52% to 18.22%. These indicate $Zn(OH)_2$, which are more hydrophilic, are formed after UV irradiation. As a result, the water CA decresaes, indicating an enhaced surface hydrophilicity. Moreover, the alkylsioxane layer from the OTS based silane coating can be decomposed by active oxygen radicals.[39] First, the reactive oxidizing species (e.g., ·OH, $O_2^{-\cdot}$, and ·OOH) generated on the ZnO surface through UV irradiation abstract hydrogen atoms from alkyl chains. Then alkoxy radicals and carbonyls are produced by continuously attacking of oxidizing specie to alkyl radicals, and they are further decomposed by photocatalysis. As a result, shorter alkyl chains are formed with loss of carbon.

One of the limitations in the application of superhydrophobic surface coatings is the poor abrasion resistance of surfaces. For example, from the previous work of our group (Table 2), the superhydrophobic silica surface was generated by sol gel method using tetramethoxysilane and isobutyltrimethox-

**Table 2. Abrasion Test of Superhydrophobic Surfaces**

| superhydrophobic surfaces | initial contact angles (deg) | initial contact angle hysteresis (deg) | contact angles after abrasion (deg) | contact angle hysteresis after abrasion (deg) |
|---|---|---|---|---|
| silica[35] | 165.4 ± 1.5 | 2–3 | 124.3 ± 5.0 | >60 |
| ZnO/epoxy nanocomposites | 158.4 ± 1.3 | 1.3 | 150.9 ± 1.0 | 25 |

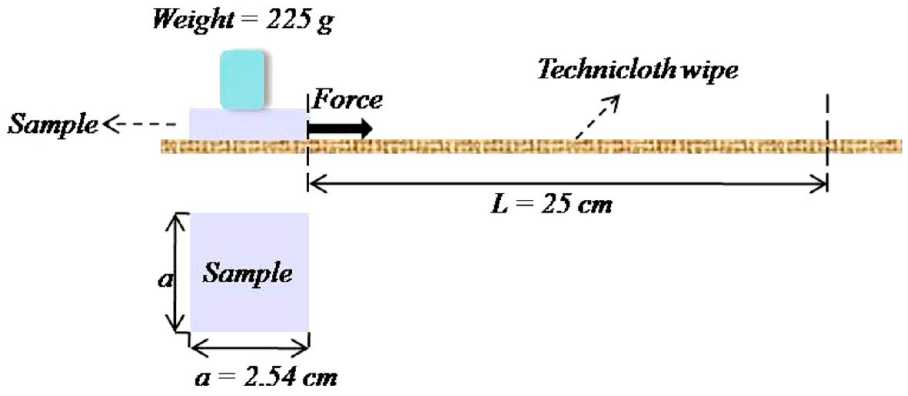


**Figure 6.** Schematic of the abrasion test employed to evaluate robustness on a superhydrophobic surface.

ysilane.[40] After abrasion test, the silica surface superhydrophobicity was lost as contact angles decreased to 124.3° and hysteresis increased to more than 60°, and the self-cleaning effect vanished. The robustness of ZnO nanocomposite was tested under a similar condition, which is schematically shown in Figure 6. It is found that the surface superhydrophobicity remained after abrasion with a contact angle of 150.9°. The possible reason is that the polymeric materials serves as stress relief layer, therefore most of the roughness was maintained in the valleys between the sub micro and nanorods. The increased contact angle hysteresis is due to the flattened top ZnO nanostructure surface. A similar mechanism was reported in our previous work about robust superhydrophobic silica epoxy nanocomposites.[41]

The reversibility of surface wettability was also realized on the ZnO nanocomposite film surface. After surface treatment of OTS, the CA recovered to 150° with CA hysteresis of ~5° and superhydrophobic surface was generated. After UV irradiation for 9 h, the surface returned to superhydrophilicity with a CA of ~0°. As shown in Figure 7, a good reversability was achived between superhydrophobicity and superhydrophilicity after repeating for five cycles. Such coating can be applied to many surfaces to realize tunable wettability for biological, chemical and electrical applications.

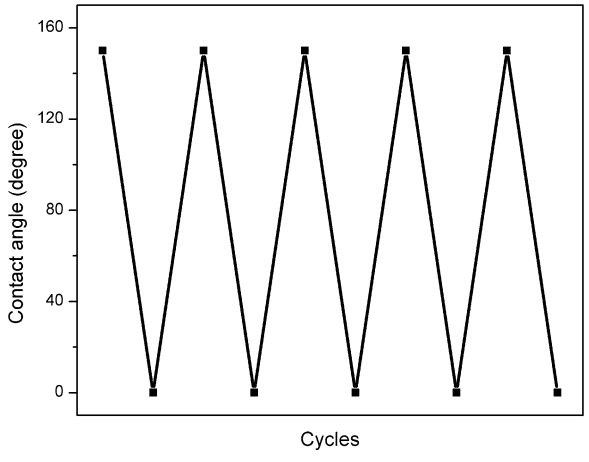


**Figure 7.** Reversible transition between superhydrophobicity induced by silane treatment and superhydrophilicity induced by UV irradiation.

## CONCLUSIONS

In summary, ZnO nanorod/epoxy composite films with tunable wettability from superhydrophobicity to superhydrophilicity were realized in our study. The composite surface exhibits hierarchical structure with both submicro and nano sized ZnO rods exposed after RIE. The surface showed superhydrophobicity by hydrophobic treatment in silane solution, and it can be transferred to superhydrophilicity by UV induced photocatalytic effect. A good reversability of wettability was achieved through cycling between UV irradiation and silane treatment. The ZnO nanocomopposite surface showed improved mechanical robustness. Such coating can be applied to many surfaces for wettability modifications, which have great potential for functional materials and devices.

## AUTHOR INFORMATION

### Corresponding Author

*Tel: 1-404-894-8391. Fax: 1-404-894-9140. E-mail: cp.wong@mse.gatech.edu.

### Notes

The authors declare no competing financial interest.

## ACKNOWLEDGMENTS

We acknowledge financial support from the National Science Foundation (NSF CMMI #0422553) and the National Electric Energy Testing Research and Applications Center (NEETRAC) at Georgia Institute of Technology. We thank Sheng Xu and Sihong Wang for their kind help and discussion.

## REFERENCES

(1) Liu, Y.; Xiu, Y. H.; Hess, D. W.; Wong, C. P. *Langmuir* **2010**, *26*, 8908.
(2) Lin, Z. Y.; Liu, Y.; Wong, C. P. *Langmuir* **2010**, *26*, 16110.
(3) Cao, L. L.; Jones, A. K.; Sikka, V. K.; Wu, J. Z.; Gao, D. *Langmuir* **2009**, *25*, 12444.

(4) Liu, Y.; Lin, W. C.; Lin, Z. Y.; Xiu, Y. H.; Wong, C. P. *Nanotechnology* **2012**, *23*, 255703.
(5) Kang, B. J.; Kim, Y. S.; Cho, Y. W.; Oh, J. H. *Microelectron. Eng.* **2011**, *88*, 2355.
(6) Takei, G.; Nonogi, M.; Hibara, A.; Kitamori, T.; Kim, H. B. *Lab Chip* **2007**, *7*, 596.
(7) Xiu, Y.; Zhu, L.; Hess, D. W.; Wong, C. P. *Nano Lett.* **2007**, *7*, 3388.
(8) Xiu, Y. H.; Liu, Y.; Hess, D. W.; Wong, C. P. *Nanotechnology* **2010**, *21*, 155705.
(9) Sinha, A. K.; Basu, M.; Pradhan, M.; Sarkar, S.; Negishi, Y.; Pal, T. *Langmuir* **2011**, *27*, 11629.
(10) Sun, R. D.; Nakajima, A.; Fujishima, A.; Watanabe, T.; Hashimoto, K. *J. Phys. Chem. B* **2001**, *105*, 1984.
(11) Feng, X. J.; Zhai, J.; Jiang, L. *Angew. Chem., Int. Ed.* **2005**, *44*, 5115.
(12) Lim, H. S.; Kwak, D.; Lee, D. Y.; Lee, S. G.; Cho, K. *J. Am. Chem. Soc.* **2007**, *129*, 4128.
(13) Zhu, W. Q.; Feng, X. J.; Feng, L.; Jiang, L. *Chem. Commun.* **2006**, 2753.
(14) Leung, K. C. F.; Xuan, S. H.; Lo, C. M. *ACS Appl. Mater. Interfaces* **2009**, *1*, 2005.
(15) Kobayashi, T.; Shimizu, K.; Kaizuma, Y.; Konishi, S. *Lab Chip* **2011**, *11*, 639.
(16) Leng, W. G.; Zhou, S. X.; Gu, G. X.; Wu, L. M. *J. Colloid Interface Sci.* **2012**, *369*, 411.
(17) Uyama, A.; Yamazoe, S.; Shigematsu, S.; Morimoto, M.; Yokojima, S.; Mayama, H.; Kojima, Y.; Nakamura, S.; Uchida, K. *Langmuir* **2011**, *27*, 6395.
(18) Tang, Z. K.; Wong, G. K. L.; Yu, P.; Kawasaki, M.; Ohtomo, A.; Koinuma, H.; Segawa, Y. *Appl. Phys. Lett.* **1998**, *72*, 3270.
(19) Huang, M. H.; Mao, S.; Feick, H.; Yan, H. Q.; Wu, Y. Y.; Kind, H.; Weber, E.; Russo, R.; Yang, P. D. *Science* **2001**, *292*, 1897.
(20) Park, W. I.; Yi, G. C. *Adv. Mater.* **2004**, *16*, 87.
(21) Lee, C. J.; Lee, T. J.; Lyu, S. C.; Zhang, Y.; Ruh, H.; Lee, H. J. *Appl. Phys. Lett.* **2002**, *81*, 3648.
(22) Zhu, Y. W.; Zhang, H. Z.; Sun, X. C.; Feng, S. Q.; Xu, J.; Zhao, Q.; Xiang, B.; Wang, R. M.; Yu, D. P. *Appl. Phys. Lett.* **2003**, *83*, 144.
(23) Xu, S.; Qin, Y.; Xu, C.; Wei, Y. G.; Yang, R. S.; Wang, Z. L. *Nat. Nanotechnol.* **2010**, *5*, 366.
(24) Wang, Z. L.; Song, J. H. *Science* **2006**, *312*, 242.
(25) Law, M.; Greene, L. E.; Johnson, J. C.; Saykally, R.; Yang, P. D. *Nat. Mater.* **2005**, *4*, 455.
(26) Liu, Y.; Das, A.; Xu, S.; Lin, Z. Y.; Xu, C.; Wang, Z. L.; Rohatgi, A.; Wong, C. P. *Adv. Energy Mater.* **2012**, *2*, 47.
(27) Xu, S.; Wang, Z. L. *Nano Res.* **2011**, *4*, 1013.
(28) Xu, B.; Cai, Z. S. *Appl. Surf. Sci.* **2008**, *254*, 5899.
(29) Liu, Y.; Lin, Z. Y.; Moon, K. S.; Wong, C. P. *Proceedings of the IEEE 61st Electronic Components Technology Conference*; IEEE: Piscataway, NJ, 2011; p 2114
(30) Liu, H.; Feng, L.; Zhai, J.; Jiang, L.; Zhu, D. B. *Langmuir* **2004**, *20*, 5659.
(31) Lv, J. G.; Zhu, J. B.; Huang, K.; Meng, F. M.; Song, X. P.; Sun, Z. Q. *Appl. Surf. Sci.* **2011**, *257*, 7534.
(32) Kumar, P. S.; Raj, A. D.; Mangalaraj, D.; Nataraj, D.; Ponpandian, N.; Li, L.; Chabrol, G. *Appl. Surf. Sci.* **2011**, *257*, 6678.
(33) Das, S. N.; Choi, J. H.; Kar, J. P.; Myoung, J. M. *Appl. Surf. Sci.* **2009**, *255*, 7319.
(34) Li, G. P.; Chen, T.; Yan, B.; Ma, Y.; Zhang, Z.; Yu, T.; Shen, Z. X.; Chen, H. Y.; Wu, T. *Appl. Phys. Lett.* 2008, *92*.
(35) Feng, X. J.; Feng, L.; Jin, M. H.; Zhai, J.; Jiang, L.; Zhu, D. B. *J. Am. Chem. Soc.* **2004**, *126*, 62.
(36) Kwak, G.; Seol, M.; Tak, Y.; Yong, K. *J. Phys. Chem. C* **2009**, *113*, 12085.
(37) Wenzel, R. N. *Ind. Eng. Chem.* **1936**, *28*, 988.
(38) Cassie, A. B. D.; Baxter, S. *Trans. Faraday Soc.* **1944**, *40*, 0546.
(39) Lee, J. P.; Kim, H. K.; Park, C. R.; Park, G.; Kwak, H. T.; Koo, S. M.; Sung, M. M. *J. Phys. Chem. B* **2003**, *107*, 8997.
(40) Xiu, Y. H.; Hess, D. W.; Wong, C. R. *J. Colloid Interface Sci.* **2008**, *326*, 465.
(41) Xiu, Y. H.; Liu, Y.; Balu, B.; Hess, D. W.; Wong, C. P. *IEEE Trans. Compon. Packag. Manuf. Technol.* **2012**, *2*, 395.